Enantioselective hydrosilylation of unsaturated carbon–heteroatom bonds (C=N, C=O) catalyzed by [Ru–S] complexes: a theoretical study†

Miao-Miao Zhou, Guanghui Chen [ID]* and Li Dang [ID]*

A detailed theoretical study on the mechanism of enanthioselective hydrosilylation of imines and ketones catalyzed by the ruthenium(II) thiolate catalyst [Ru–S] ([L*-Ru(SDmp)]⁺[BAr₄ᶠ]⁻) with a chiral monodentate phosphine ligand is carried out in this work. We elucidate all the pathways leading to the main products or by products mediated by the [Ru–S] complex in order to have deep understanding of the chemoselectivity and enantioselectivity. The DFT (Density Functional Theory) calculations show that the reaction mechanism including: (1) Si–H bond cleavage by the dual activity of Ru–S bond; (2) the generation of a sulfur-stabilized silane cation; (3) the electrophilic attack of silane cation to N=C/O=C; (4) hydrogen transfer from Ru to carbon cation. The hydrosilylation products are found to be the final products rather than the dehydrogenative ones, which is consistent with the experimental results. The dehydrogenative silylation reaction pathways which give N- or O-silylated enamine/enol ether are reversible according to our calculations. The computational results also show that the electrophilic attack of silicon to N=C/O=C is the rate-determining step and the ee value can be improved significantly with more bulky model phosphine ligand based on the same calculation methods.

Introduction

Nowadays, the demand for enantiomerically pure compounds is increasing gradually in the fields of biochemistry and pharmaceutical chemistry.[1] Chiral alcohols and amines are common organic compounds as important building blocks for organic synthesis.[2] The asymmetric reduction of unsaturated compounds, such as ketones and imines, remains one of the fundamental approaches to synthesize biologically active agents and pharmaceutical products in the laboratory and industry.[3,4] At the same time, silanes have been developed as an alternative to hydrogenation reagents because the H–Si bond is easier to be heterolytically splitted by catalysts than H–H bonds in organic synthesis.[5] Furthermore, hydrosilylation reactions play a crucial role across industrial fields due to the easily handled, low cost and non-toxic characteristics of silicon reagents,[6] together with the mild reaction conditions required and various applications. The silyl group is also retained as a protecting group to facilitate further functionalization of the reaction products.[7,8] Currently, the asymmetric hydrosilylation of prochiral ketones and imines

has been investigated by using transition metal catalysts, such as Rh,[9] Ir,[10] Co,[11] Fe,[12] Ru[13a,c,d] and so on.

In order to make progress in asymmetric catalytic hydrosilylation of ketones and imines, low reaction activity, narrow substrate range, harsh reaction conditions and difficult recovery of catalysts need to be overcome, great progress and important breakthroughs need to be made in the challenging hydrosilylation of ketones and imines.[13] Interestingly, in the hydrosilylation of ketones, rhodium catalysts can reach more than 90% ee for a broad spectrum of substrates despite a reaction temperature of about −60 °C.[14] Cobalt(III) complexes have also been used as catalysts for this reaction but require temperatures of 60 °C and long reaction times to give the final products.[15] In 2019, Koga and coworkers explored the mechanism of hydrosilylation of imines by using iron catalysts.[16a] An iron three membered ring intermediate was suggested.[16a] Hasegawa's group investigated the Rh-catalyzed hydrosilylation of acetone or ethylene with tertiary silane to examine three existing mechanisms, the Chalk–Harrod (CH) mechanism, the modified Chalk–Harrod (mCH) mechanism, and the outer-sphere mechanism.[16b] They also proposed another two reaction pathways, the double hydride (DH) mechanism and the alternative Chalk–Harrod (aCH) mechanism.[16b] It was found that the entire hydrosilylation reaction takes place only at the center of the reaction, without the participation of the ligand. Single active site catalysts can be used for the molecular catalysts, but also for periodic surface catalysis. The 2D materials are a platform to design efficient single active site catalysts for various reactions.[17]

Department of Chemistry, Key Laboratory for Preparation and Application of Ordered Structural Materials of Guangdong Province, Shantou University, Guangdong 515063, P. R. China. E-mail: ldang@stu.edu.cn; ghchen@stu.edu.cn

Moreover, coordinatively unsaturated ruthenium(II) thiolate complexes with bulky ligands reported by Tatsumi and Oestreich have been used in the cooperative activation of H–H bonds,[18] Si–H bonds,[19] B–H bonds[20] and Al–H bonds.[21] Based on these works, the Oestreich group changed the phosphine ligand to a chiral monodentate phosphine ligand to achieve enantioselective hydrosilylation of enolizable imines and ketones, which provided the corresponding chiral products at low catalyst loadings (as low as 1 mol%) at room temperature and with no additives.[22] Differently, in the Ru–S catalyzed hydrosilylation reaction, it is assumed that the transition metal Ru shows Lewis acidity while the thiolate ligand works as the Lewis base to split X–H (X = B, Al, Si) bonds. That is to say, the [Ru–S] complex was performed bifunctional catalytic activation. Although (*S*)-silyl amines and (*S*)-silyl ethers were observed as the major products, but the ee value is not very high. Intrigued by these experimental results, we are interested in studying the mechanism of Ru–S cooperatively catalyzed enantioselective hydrosilylation of imines and ketones, in order to confirm the role of basic thiolate ligand in these reactions and investigate the methods to improve the ee value.

Computational details

Gaussian 16 [23] was used for all calculations in this work. Geometric structures optimization and frequency calculation were conducted by M062X[24] functional in gas phase at $T = 298.15$ K and 1 atm pressure. The LANL2DZ basis set was used for Ru atom[25] with the polarization functions added for Ru ($f = 1.235$).[26] The all-electron basis set 6-31G[27] was used in describing the atoms (C, H, O, N, P, S). There is no imaginary frequency for all the intermediates while only-one imaginary frequency is in transition state (**TS**) structures. In addition, the intrinsic reaction coordinate (IRC) calculation[28] which correctly bridged the intermediates further demonstrate the credibility of transition state structures. Based on the gas-phase optimized geometries, solvation effect of toluene was incorporated with the SMD[29] model at the level of B3LYP-D3 [30] while LANL2DZ basis set for Ru atom and 6-311++G** basis set for all other main group atoms. We used simplified Si reagent PhSiH$_3$ rather than PhMeSiH$_2$ to avoid the overestimation of the steric effect from reactant. All 3D molecular structures were generated by using the CYLview (Version) program.[31] The numbers shown in energy profiles are solvent corrected Gibbs free energies based on SMD model.

Results and discussion

Based on the experimental observation, we studied the reaction mechanism of the Ru–S catalyzed hydrosilylation of imines and ketones in order to understand better on the dual role of Ru–S catalyst and how the enantioselectivity is controlled by using bulky ligand on Ru–S catalyst.[22] Since imines and ketones can react with silanes to give hydrosilylation and dehydrogenative silylation products as shown in Scheme 1. Reactions of imines and ketones with silanes promoted by catalyst **I1** can have reaction pathways: (1) the cleavage of Si–H bond by Ru–S bond;
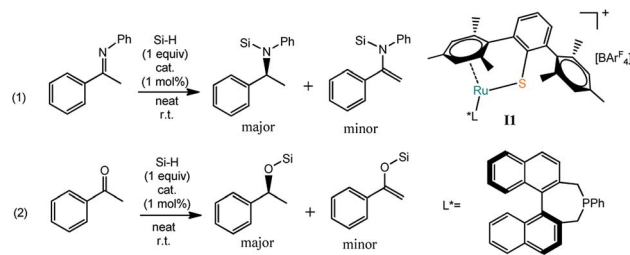
Scheme 1 Hydrosilylation or dehydrogenative silylation of imine and ketone catalyzed by [Ru–S] complex (left) and the structure of [Ru–S] catalyst **I1** and **L*** (right).
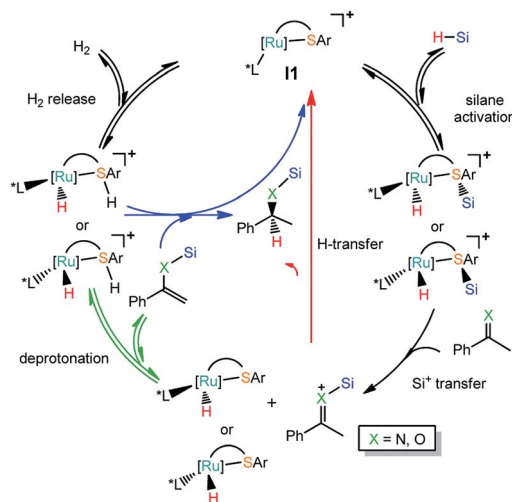
Scheme 2 Reactions pathways for Ru thiolate complex catalyzed hydrosilylation (red line) or dehydrogenative silylation of imine and ketone (green line).

(2) silyl group transfer from S to X (X = N, O); (3) hydrogen transfer from Ru to carbon of imine or ketone or proton transfer from imine or ketone to sulfur ligand; (4) [Ru–S] complex regeneration through H$_2$ release or hydrogenation reaction of alkenyl silane (Scheme 2). The detailed mechanism of these pathways will be studied and discussed and the origin of the competition between hydrosilylation and dehydrogenative silylation reactions is addressed. Unless specified, all the figures of the potential energy profiles are presented in the relative Gibbs free energies in solution (kcal mol^{-1}). The relative Gibbs free energies and electronic energies in gas-phase are shown in Table S1 (see ESI† for details). The relative Gibbs free energies and relative electronic energies in gas-phase are similar in cases when the number of the reactant and product molecules is equal, for example, one-to-one or two-to-two transformations. However, this differs significantly for one-to-two or two-to-one transformations because of the entropic contribution.

Free energy profile for **I1** catalyzed hydrosilylation of imine is shown in Fig. 1. The catalytic reaction is triggered by the coordination of silane on Ru center to form intermediate **I2**. Then, H–Si bond is splitted heterolytically by Ru–S bond, which undergoes silane activation process *via* a silicon-stabilized
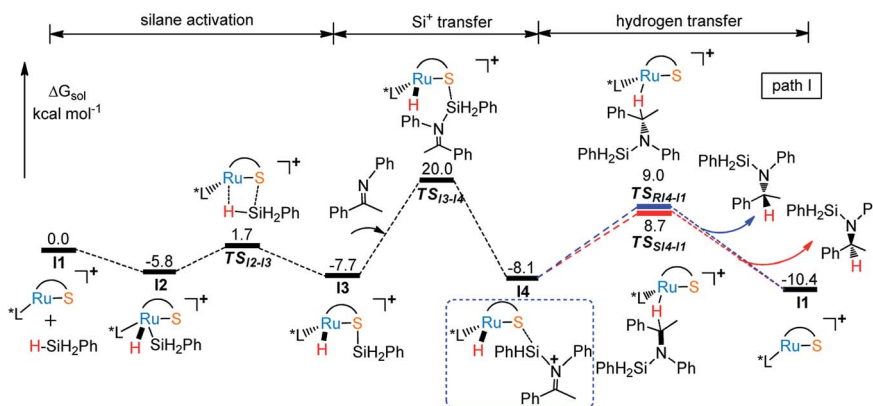
Fig. 1 Free energy profile for **I1** catalyzed hydrosilylation of imine by route 1.
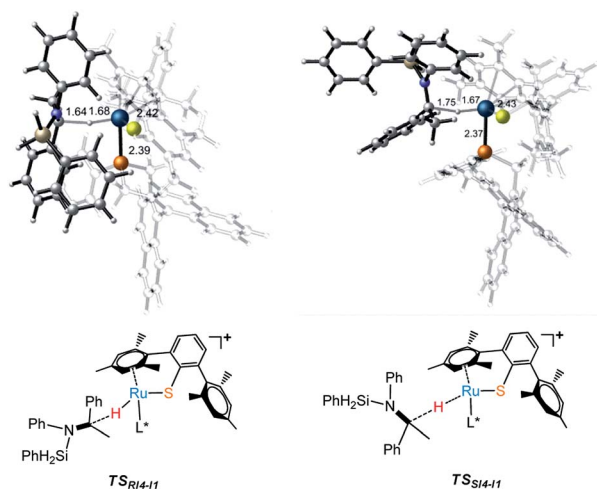

Fig. 2 Transition states (TSs) for the formation of *R*- and *S*- alkyl silyl amines.

quadrilateral transition state **TS$_{I2-I3}$** ($\Delta G^{\ddagger}$ = 7.5 kcal mol^{-1}) to give a silicon electrophile and a metal hydride due to the Lewis acidic Ru center and basic thiolate ligand. Next, the silyl group migrates from S to N of imine through transition state **TS$_{I3-I4}$** with a free energy barrier of 27.7 kcal mol^{-1}, which is the rate determining step of the whole reaction. After that, the hydride on Ru transfers to silyl imide cation with enantioselectivity. At last, *R*- and *S*-silyl amines are generated by the transition states **TS$_{RI4-I1}$** and **TS$_{SI4-I1}$** with the energy barriers 17.1 kcal mol^{-1} and 16.8 kcal mol^{-1}, respectively. Therefore, S-silyl amine is the main product in the whole reaction with 24.79% ee by calculation. Taking a close look at the structures of transition states **TS$_{RI4-I1}$** and **TS$_{SI4-I1}$**, we found that the repulsion between amine group and phosphine ligand is larger in **TS$_{RI4-I1}$** than that between methyl group and phosphine ligand in **TS$_{SI4-I1}$**, leading to lower energy of **TS$_{SI4-I1}$** (Fig. 2).

Considering the basicity of thiolate ligand, a possible reaction pathway is the proton transfer from silyl imide cation to S
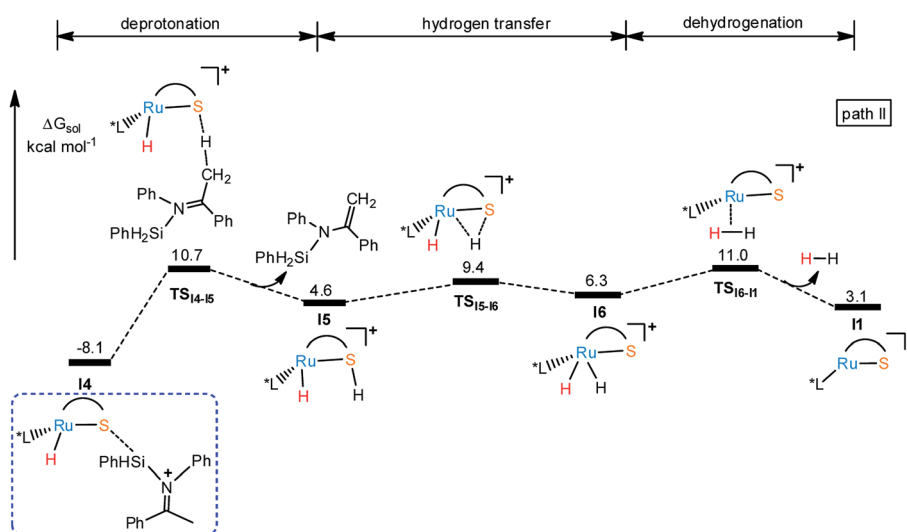

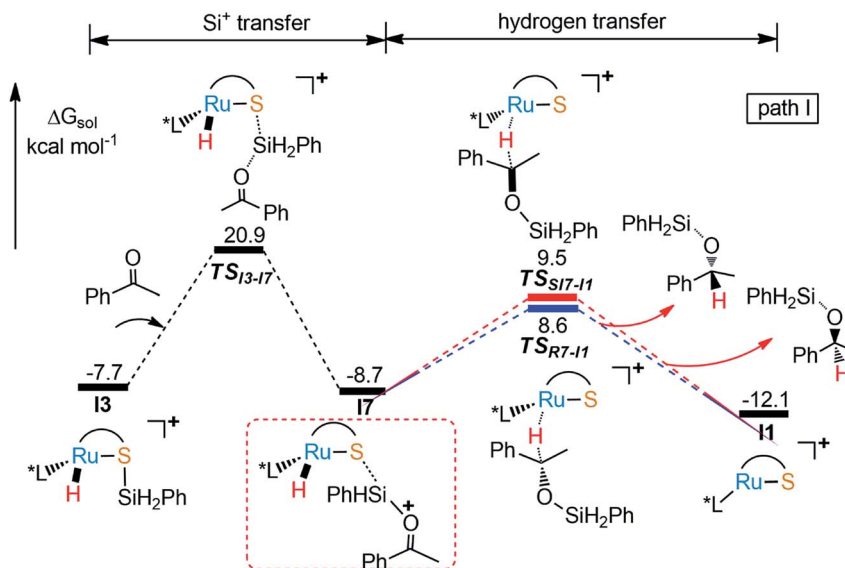**Fig. 3** Free energy profile for **I1** catalyzed dehydrogenative silylation of imine.

Fig. 4 Free energy profile for **I1** catalyzed hydrosilylation of ketone.

in **I4** through transition state **TS$_{I4\text{-}I5}$** (18.8 kcal mol^{-1} energy barrier) to release silyl enamine and generate intermediate **I5** as shown in Fig. 3. And hydrogen elimination takes place through transition state **TS$_{I5\text{-}I6}$** ($\Delta G^{\ddagger} = 17.5$ kcal mol^{-1}) to give intermediate **I6**. At last, dehydrogenation happens to regenerate **I1** via the **TS$_{I6\text{-}I1}$** with the barrier of 19.1 kcal mol^{-1}, finishing the catalytic cycle. Although the reaction barriers for all these processes are low, the whole reaction is endothermic, about 3.1 kcal mol^{-1}, which makes the pathway in Fig. 4 thermodynamically unfavorable. In summary, the main product of this reaction can be silyl amine instead of silyl enamine.

As part of the ongoing effort to explore the reduction of aryl ketone. Similar to the calculation of Ru–S catalyzed reaction of imine with silane, we also study the reaction mechanism of

ketone with PhSiH$_3$. As shown in Fig. 4, when **I3** reacts with ketone, silyl group migrates from **I3** to O of keto to give **I7** via a very high energy barrier (**TS$_{I3\text{-}I7}$**, $\Delta G^{\ddagger} = 28.6$ kcal mol^{-1}), which is also the rate determining step of the whole reaction. After that, the hydride transfer from Ru to carbonyl carbon to give R- and S-silyl ether through transition states **TS$_{RI7\text{-}I1}$** and **TS$_{SI7\text{-}I1}$** with the energy barriers 17.3 kcal mol^{-1} and 18.2 kcal mol^{-1}, respectively. Here, the calculation results show that the formation of R- and S-silyl ether have similar reaction barriers resulting of moderate enantioselectivity of products, about 64.08% ee of R-silyl ether. Taking a close look at the structures of transition states **TS$_{RI7\text{-}I1}$** and **TS$_{SI7\text{-}I1}$**, we found that the repulsion between silyl ether group and phosphine ligand in **TS$_{RI7\text{-}I1}$** and the repulsion between phenyl group and phosphine ligand in **TS$_{SI7\text{-}I1}$** are all not obvious, leading to similar energy of **TS$_{RI7\text{-}I1}$** and **TS$_{SI7\text{-}I1}$** (Fig. 5).

In the same way, there is another reaction pathway from intermediate **I7** when considering the Lewis basicity of sulfur ligand. As shown in Fig. 6, hydrogen transfer from methyl group to sulfur occurs because of the electronegativity of thiolate ligand resulting in the formation of **I5** and release the alkenyl silyl ether. **I6** is generated through transition state **TS$_{I5\text{-}I6}$** with the energy barrier 17.9 kcal mol^{-1} by transferring hydrogen from S to Ru. At last, reductive elimination occurs to regenerate **I1** and release dihydrogen via **TS$_{I6\text{-}I1}$** with the energy barrier 19.4 kcal mol^{-1}. Similar to dehydrogenative silylation of imine, the reaction pathway in Fig. 4 is endothermic, which makes the dehydrogenative silylation of ketone thermodynamically unfavorable. Therefore, the main product of this Ru–S cooperatively catalyzed reaction is silyl ether instead of silyl-ketene.

When the phosphine ligand is changed from **L*** to P(iso-butanyl)$_3$, the energy difference between R- and S- transition states (**TS**s) became larger and enantioselectivity is enhanced a lot (Fig. 7). Comparing the structural character of transition states **TS$_{RI9\text{-}I1}$**, **TS$_{SI9\text{-}I1}$**, **TS$_{RI10\text{-}I1}$** and **TS$_{SI10\text{-}I1}$**, the repulsion
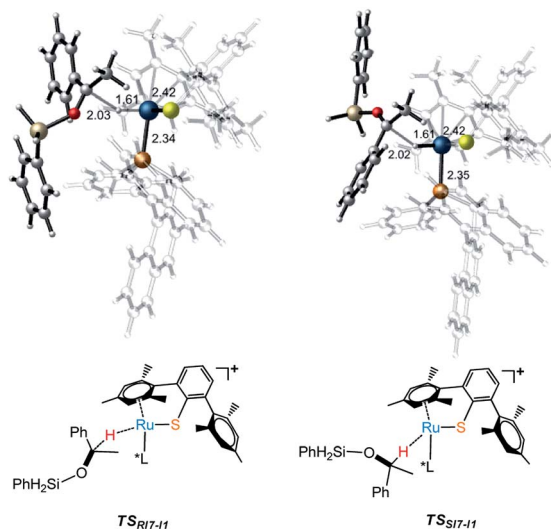

Fig. 5 Transition states (TSs) for the formation of R- and S- alkyl silyl ethers.
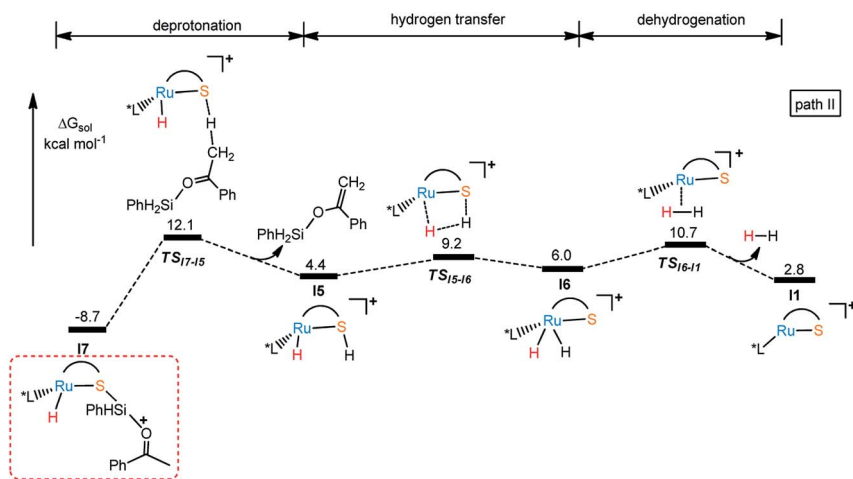
Fig. 6 Free energy profile for **I1** catalyzed dehydrogenative silylation of ketone.
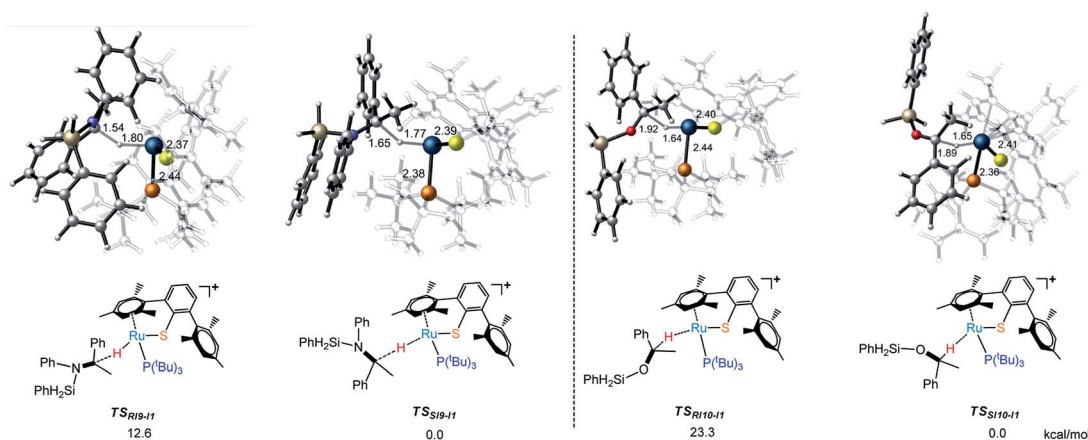

Fig. 7 Transition states (**TS**s) for the formation of *R*- and *S*- alkyl silyl amine and ether catalyzed by [RuS]P(^{t}Bu)$^+$.

between silyl group and phosphine ligand in **TS$_{RI9-I1}$** and **TS$_{RI10-I1}$** is much larger than the repulsion between phenyl group and phosphine ligand in **TS$_{SI9-I1}$** and **TS$_{SI10-I1}$**, which explains the ee value predicted from model ligand P(iso-butanyl)$_3$. The larger repulsion makes the transition state more distorted, which destabilizes the **TS$_{RI9-I1}$** and **TS$_{RI10-I1}$**,[32] while for catalysts with smaller repulsion in **TS**, the attractive, dynamic, and cooperative non-covalent interactions can make other *R*- and *S*- transition states have similar flexibility and stability.[32d]

Conclusion

In summary, we set out to elucidate the mechanism of the [Ru–S] complex as catalysts for hydrosilylation of ketones and imines and explain the chemo- and enantio-selectivity involved in these reactions. In the catalytic process, the [Ru–S] complex is assumed to play a decisive role by heterolytically splitting the Si–H bond to form a sulfur-stabilized ruthenium hydride intermediate and a Si electrophile that can attract electron rich N and O atoms to form a cation. Although both hydro-silylation and dehydrogenative silylation processes afterward

have barriers less than 30 kcal mol^{-1}, the dehydrogenative silylation is reversible, making this pathway unfavourable. At the same time, the regioselectivity of these reactions is not high according to our calculations, we can predict that a bulky phosphine ligand such as P(iso-butanyl)$_3$ can enhance the enantioselectivity significantly.

Conflicts of interest

There are no conflicts to declare.

Acknowledgements

Notes and references

1 (a) M. P. Schneider and U. Goergens, *Tetrahedron: Asymmetry*, 1992, **3**, 525–528; (b) R. K. Pandey, R. A. Fernandes and P. Kumar, *Tetrahedron Lett.*, 2002, **43**,

4425–4426; (*c*) X. Xu, R. Fu, J. Chen, S. Chen and X. Bai, *Bioorg. Med. Chem. Lett.*, 2007, **17**, 101–104; (*d*) D. J. Wardrop and J. Fritz, *Org. Lett.*, 2006, **8**, 3659–3662; (*e*) J. D. Katz, J. P. Jewell, D. J. Guerin, J. Lim, C. J. Dinsmore, S. V. Deshmukh, B. S. Pan, C. G. Marshall, W. Lu and M. D. Altman, *J. Med. Chem.*, 2011, **54**, 4092–4108.

2 (*a*) G. Zanoni, A. Porta, Q. D. Toma, F. Castronovo and G. Vidari, *J. Org. Chem.*, 2003, **68**, 6437–6439; (*b*) P. Hoyos, J. V. Sinisterra, F. Molinari and A. R. Alcántara, *Acc. Chem. Res.*, 2010, **43**, 288–299; (*c*) B. M. Trost, I. Fleming and C. H. Heathcock, *Comprehensive Organic Synthesis*, Pergamon, Oxford, 1991, vol. 2, pp. 1–53; (*d*) T. Mukaiyama, *Tetrahedron*, 1999, **55**, 8609–8670; (*e*) K. C. Nicolaou, D. Vourloumis, N. Winssinger and P. S. Baran, *Angew. Chem., Int. Ed.*, 2000, **39**, 44–122; (*f*) D. A. Evans, A. M. Ratz, B. E. Huff and G. S. Sheppard, *J. Am. Chem. Soc.*, 1995, **117**, 3448–3467; (*g*) B. Schetter and R. Mahrwald, *Angew. Chem., Int. Ed.*, 2006, **45**, 7506–7525; (*h*) I. Paterson and M. M. Mansuri, *Tetrahedron*, 1985, **41**, 3569–3624; (*i*) S. Masamune, G. S. Bates and J. W. Corcoran, *Angew. Chem., Int. Ed.*, 1977, **16**, 585–607.

3 (*a*) P. J. Harrington and E. Lodewijk, *Org. Process Res. Dev.*, 1997, **1**, 72–76; (*b*) X. Chen, J. Z. Fong, J. Xu, C. Mou, Y. Lu, S. Yang, B. A. Song and Y. R. Chi, *J. Am. Chem. Soc.*, 2016, **138**, 7212–7215; (*c*) C. Chen, H. Wang, Z. Zhang, S. Jin, S. Wen, J. Ji, L. W. Chung, X. Q. Dong and X. Zhang, *Chem. Sci.*, 2016, **7**, 6669–6673; (*d*) S. F. Zhu, Y. Cai, H. X. Mao, J. H. Xie and Q. L. Zhou, *Nat. Chem.*, 2010, **2**, 546–551; (*e*) M. Breuer, K. Ditrich, T. Habicher, B. Hauer, M. Keßeler, R. Stürmer and T. Zelinski, *Angew. Chem., Int. Ed.*, 2004, **43**, 788–824; (*f*) L. Sutin, S. Anderson, L. Bergquist, V. M. Castro, E. Danielsson, S. James, M. Henriksson, L. Johansson, C. Kaiser, K. Flyren and M. Williams, *Bioorg. Med. Chem. Lett.*, 2007, **17**, 4837–4840.

4 (*a*) S. Lou and C. Fu, *J. Am. Chem. Soc.*, 2010, **132**, 1264–1266; (*b*) P. M. Lundin, J. Esquivias and C. Fu, *Angew. Chem., Int. Ed.*, 2009, **121**, 160–162; (*c*) A. H. Cherney, N. T. Kadunce and S. E. Reisman, *J. Am. Chem. Soc.*, 2013, **135**, 7442–7445.

5 (*a*) J. M. Brunel, *Int. J. Hydrogen Energy*, 2010, **35**, 3401–3405; (*b*) J. M. Brunel, *Int. J. Hydrogen Energy*, 2017, **42**, 23004–23009.

6 F. Meinardi, S. Ehrenberg, L. Dhamo, F. Carulli, M. Mauri, F. Bruni, R. Simonutti, U. Kortshagen and S. Brovelli, *Nat. Photon.*, 2017, **11**, 177–185.

7 (*a*) M. C. Pirrung, L. Fallon, J. Zhu and Y. R. Lee, *J. Am. Chem. Soc.*, 2001, **123**, 3638–3643; (*b*) M. Parasram and V. Gevorgyan, *Acc. Chem. Res.*, 2017, **50**, 2038–2053.

8 (*a*) T. Murai, T. Sakane and S. Kato, *J. Org. Chem.*, 1990, **55**, 449–453; (*b*) A. C. Fernandes and C. C. Romao, *Tetrahedron Lett.*, 2005, **46**, 8881–8883; (*c*) A. C. Fernandes and C. C. Romao, *J. Mol. Catal. A: Chem.*, 2007, **272**, 60–63; (*d*) R. G. Noronha, A. C. Fernandes and C. C. Romao, *Tetrahedron Lett.*, 2009, **50**, 1407–1410; (*e*) R. G. Noronha, C. C. Romao and A. C. Fernandes, *J. Org. Chem.*, 2009, **74**, 6960–6964; (*f*) R. G. Noronha, C. C. Romao and A. C. Fernandes, *Catal. Commun.*, 2011, **12**, 337–340; (*g*) G. Du and P. E. Fanwick, *Inorg. Chim. Acta*, 2008, **361**,

3184–3192; (*h*) K. A. Nolin, R. W. Ahn, Y. Kobayashi, J. J. Kennedy-Smith and F. D. Toste, *Chem.–Eur. J.*, 2010, **16**, 9555–9562; (*i*) G. I. Nikonov and D. V. Gutsulyak, *Angew. Chem., Int. Ed.*, 2010, **49**, 7553–7556.

9 (*a*) K. Riener, M. P. Högerl, P. Gigler and F. E. Kühn, *ACS Catal.*, 2012, **2**, 613–621; (*b*) I. Ojima, M. Kogure and M. Kumagai, *J. Org. Chem.*, 1977, **42**, 1671–1679; (*c*) M. Sawamura, R. Kuwano and Y. Ito, *Angew. Chem., Int. Ed.*, 1994, **33**, 111–113; (*d*) D. Enders, H. Gielen and K. Breuer, *Tetrahedron: Asymmetry*, 1997, **8**, 3571–3574; (*e*) K. Kromm, P. L. Osburn and L. Gladysz, *Organometallics*, 2002, **21**, 4275–4280; (*f*) D. A. Evans, E. M. Forrest, J. S. Tedrow and K. R. Campos, *J. Am. Chem. Soc.*, 2003, **125**, 3534–3543; (*g*) W. L. Duan, M. Shi and G. B. Rong, *Chem. Commun.*, 2003, **35**, 2916–2917; (*h*) C. G. Arena and R. J. Pattacini, *J. Mol. Catal. A: Chem.*, 2004, **222**, 47–52; (*i*) V. Cesar, S. Bellemin-Laponnaz, H. Wadepohl and L. H. Gade, *Chem.–Eur. J.*, 2005, **11**, 2862–2873; (*j*) T. Imamoto, T. Itoh, Y. Yamanoi, R. Narui and K. Yoshida, *Tetrahedron: Asymmetry*, 2006, **17**, 560–565; (*k*) N. Schneider, M. Finger, C. Haferkemper, S. Bellemin-Laponnaz, P. Hofmann and L. H. Gade, *Angew. Chem., Int. Ed.*, 2009, **48**, 1609–1613; (*l*) N. Schneider, M. Finger, C. Haferkemper, S. Bellemin-Laponnaz, P. Hofmann and L. H. Gade, *Chem.–Eur. J.*, 2010, **15**, 11515–11529; (*m*) N. Schneider, M. Kruck, S. Bellemin-Laponnaz, H. Wadepohl and L. H. Gade, *Eur. J. Inorg. Chem.*, 2009, **4**, 493–500.

10 (*a*) R. Malacea, R. Poli and E. Manoury, *Coord. Chem. Rev.*, 2010, **254**, 729–752; (*b*) R. S. Tanke and R. H. Crabtree, *J. Am. Chem. Soc.*, 1990, **112**, 7984–7989; (*c*) S. Doherty, J. G. Knight, T. H. Scanlan, M. R. J. Elsegood and W. J. Clegg, *Organomet. Chem.*, 2002, **650**, 231–248; (*d*) M. Martín, E. Sola, O. Torres, P. Pablo and L. A. Oro, *Organometallics*, 2003, **22**, 5406–5417; (*e*) S. R. Klei, T. D. Tilley and R. G. Bergman, *Organometallics*, 2002, **21**, 4648–4661; (*f*) L. D. Field, B. A. Messerle and S. L. Wren, *Organometallics*, 2003, **22**, 4393–4395.

11 (*a*) H. Brunner, R. Becker and G. Rielp, *Organometallics*, 1984, **3**, 1354–1359; (*b*) L. H. Gade, V. Cesar and S. Bellemin-Laponnaz, *Angew. Chem., Int. Ed.*, 2004, **43**, 1014–1017; (*c*) L. M. Newman, J. M. J. Williams, R. McCague and G. A. Potter, *Tetrahedron: Asymmetry*, 1996, **7**, 1597–1598; (*d*) T. Langer, J. Janssen and G. Helmchen, *Tetrahedron: Asymmetry*, 1996, **7**, 1599–1602; (*e*) B. Tao and G. C. Fu, *Angew. Chem., Int. Ed.*, 2002, **41**, 3892–3894.

12 (*a*) X. Sun, L. Zhou, W. Li and X. Zhang, *J. Org. Chem.*, 2008, **73**, 1143–1146; (*b*) S. Otocka, M. Kwiatkowska, L. Madalińska and P. Kiełbasiński, *Chem. Rev.*, 2017, **117**, 4147–4181; (*c*) C. Kan, J. Hu, Y. Huang, H. Wang and H. Ma, *Macromolecules*, 2017, **50**, 7911–7919; (*d*) Y. Deng, C. V. Karunaratne, E. Csatary, D. L. Tierney, K. Wheeler and H. Wang, *J. Org. Chem.*, 2015, **80**, 7984–7993; (*e*) H. Teng, Y. Luo, M. Nishiura and Z. Hou, *J. Am. Chem. Soc.*, 2017, **139**, 16506–16509; (*f*) F. S. Wekesa, R. Arias-Ugarte, L. Kong, Z. Sumner, G. P. McGovern and

M. Findlater, *Organometallics*, 2015, **34**, 5051–5056; (*g*) A. Kišić, M. Stephan and B. Mohara, *Adv. Synth. Catal.*, 2015, **357**, 2540–2546; (*h*) B. Tao and G. C. Fu, *Angew. Chem., Int. Ed.*, 2002, **41**, 3892–3894; (*i*) I. Takei, Y. Nishibayashi, Y. Ishii, Y. Mizobe, S. Uemura and M. Hidai, *Chem. Commun.*, 2001, 2360–2361; (*j*) S. Hosokawa, J. I. Ito and H. Nishiyama, *Organometallics*, 2010, **29**, 5773–5775.

13 (*a*) M. L. Huw, C. V. Davies, H. Tore and W. H. Darrin, *J. Am. Chem. Soc.*, 2003, **125**, 6462–6468; (*b*) J. W. Patrick, *Acc. Chem. Res.*, 2003, **36**, 739–749; (*c*) Y. Nishibayashi, I. Takei, S. Uemura and M. Hidai, *Organometallics*, 1998, **17**, 3420–3422; (*d*) B. Li, J. Sortais, C. Darcel and P. H. Dixneuf, *ChemSusChem*, 2012, **5**, 396–399; (*e*) C. Song, C. Ma, Y. Ma, W. Feng, S. Ma, Q. Chai and M. B. Andrus, *Tetrahedron Lett.*, 2005, **46**, 3241–3244.

14 V. César, S. Bellemin-Laponnaz and L. H. Gade, *Angew. Chem., Int. Ed.*, 2004, **43**, 1014–1017.

15 H. Zhou, H. Sun, S. Zhang and X. Li, *Organometallics*, 2015, **34**, 1479–1486.

16 (*a*) A. A. Dahy and N. Koga, *J. Comput. Chem.*, 2019, **40**, 62–71; (*b*) L. Zhao, N. Nakatani, Y. Sunada, *et al.*, *J. Org. Chem.*, 2019, **84**, 8552–8561.

17 (*a*) B. Song, Y. Zhou, H.-M. Yang, J.-H. Liao, L.-M. Yang, X.-B. Yang and E. Ganz, *J. Am. Chem. Soc.*, 2019, **141**, 3630–3640; (*b*) J.-H. Liu, L.-M. Yang and E. Ganz, *J. Mater. Chem. A*, 2019, **7**, 3805–3814; (*c*) J.-H. Liu, L.-M. Yang and E. Ganz, *J. Mater. Chem. A*, 2019, **7**, 11944–11952; (*d*) J.-H. Liu, L.-M. Yang and E. Ganz, *RSC Adv.*, 2019, **9**, 27710–27719; (*e*) J.-H. Liu, L.-M. Yang and E. Ganz, *Energy Environ. Mater.*, 2019, **2**, 193–200; (*f*) J. H. Liu, L. M. Yang and E. Ganz, *ACS Sustainable Chem. Eng.*, 2018, **6**, 15494–15502; (*g*) L. Xu, L.-M. Yang and E. Ganz, *Theor. Chem. Acc.*, 2018, **137**, 98; (*h*) L.-M. Yang, V. Bacic, I. A. Popov, A. I. Boldyrev, T. Heine, T. Frauenheim and E. Ganz, *J. Am. Chem. Soc.*, 2015, **137**, 2757–2762.

18 (*a*) Y. Ohki, Y. Takikawa, H. Sadohara, C. Kesenheimer, B. Engendahl, E. Kapatina and K. Tatsumi, *Chem.–Asian J.*, 2008, **3**, 1625–1635; (*b*) A. Lefranc, Z. W. Qu, S. Grimme and M. Oestreich, *Chem.–Eur. J.*, 2016, **22**, 10009–10016.

19 (*a*) T. Stahl, K. Müther, Y. Ohki, K. Tatsumi and M. Oestreich, *J. Am. Chem. Soc.*, 2013, **135**, 10978–10981; (*b*) T. Stahl, H. F. T. Klare and M. Oestreich, *J. Am. Chem. Soc.*, 2013, **135**, 1248–1251.

20 T. Stahl, K. Müther, Y. Ohki, K. Tatsumi and M. Oestreich, *J. Am. Chem. Soc.*, 2013, **135**, 10978–10981.

21 F. Forster, T. T. Metsanen, E. Irran, P. Hrobarik and M. Oestreich, *J. Am. Chem. Soc.*, 2017, **139**, 16334–16342.

22 S. Bahr and M. Oestreich, *Organometallics*, 2017, **36**, 935–943.

23 M. J. Frisch, G. W. Trucks, H. B. Schlegel, G. E. Scuseria, M. A. Robb, J. R. Cheeseman, G. Scalmani, V. Barone, G. A. Petersson, H. Nakatsuji, X. Li, M. Caricato, A. V. Marenich, J. Bloino, B. G. Janesko, R. Gomperts, B. Mennucci, H. P. Hratchian, J. V. Ortiz, A. F. Izmaylov, J. L. Sonnenberg, D. Williams-Young, F. Ding, F. Lipparini, F. Egidi, J. Goings, B. Peng, A. Petrone, T. Henderson, D. Ranasinghe, V. G. Zakrzewski, J. Gao, N. Rega, G. Zheng, W. Liang, M. Hada, M. Ehara, K. Toyota, R. Fukuda, J. Hasegawa, M. Ishida, T. Nakajima, Y. Honda, O. Kitao, H. Nakai, T. Vreven, K. Throssell, J. A. Montgomery Jr, J. E. Peralta, F. Ogliaro, M. J. Bearpark, J. J. Heyd, E. N. Brothers, K. N. Kudin, V. N. Staroverov, T. A. Keith, R. Kobayashi, J. Normand, K. Raghavachari, A. P. Rendell, J. C. Burant, S. S. Iyengar, J. Tomasi, M. Cossi, J. M. Millam, M. Klene, C. Adamo, R. Cammi, J. W. Ochterski, R. L. Martin, K. Morokuma, O. Farkas, J. B. Foresman, and D. J. Fox, Gaussian, Inc., Wallingford CT, 2016.

24 (*a*) Y. Zhao and D. G. Truhlar, *Theor. Chem. Acc.*, 2008, **120**, 215–241; (*b*) Y. Zhao and D. G. Truhlar, *J. Phys. Chem. A*, 2006, **110**, 13126–13130; (*c*) Y. Zhao and D. G. Truhlar, *J. Chem. Phys.*, 2006, **125**, 194101–194120; (*d*) S. Grimme, *J. Comput. Chem.*, 2006, **27**, 1787–1799.

25 (*a*) A. D. Becke, *J. Chem. Phys.*, 1993, **98**, 5648–5652; (*b*) C. Lee, W. Yang and R. G. Parr, *Phys. Rev. B: Condens. Matter Mater. Phys.*, 1988, **37**, 785–789; (*c*) P. J. Hay and W. R. Wadt, *J. Chem. Phys.*, 1985, **82**, 299–310.

26 (*a*) A. W. Ehlers, M. Biihme, S. Dapprich, A. Gobbi, A. Hijllwarth, V. Jonas, K. F. Kiihler, R. Stegmann, A. Veldkamp and G. Frenking, *Chem. Phys. Lett.*, 1993, **208**, 111–114; (*b*) A. Höllwarth, M. Böhme, S. Dapprich, A. W. Ehlers, A. Gobbi, V. Jonas, K. F. Köhler, R. Stegmann, A. Veldkamp and G. Frenking, *Chem. Phys. Lett.*, 1993, **208**, 237–240.

27 G. A. Petersson, A. Bennett, T. G. Tensfeldt, M. A. Al-Laham, W. A. Shirley and J. J. Mantzaris, *Chem. Phys.*, 1988, **89**, 2193–2218.

28 C. Gonzalez and H. B. Gonzalez, *J. Phys. Chem.*, 1990, **94**, 5523–5527.

29 A. V. Marenich, C. J. Cramer and D. G. Truhlar, *J. Phys. Chem. B*, 2009, **113**, 6378–6396.

30 (*a*) S. Grimme, J. Antony, S. Ehrlich and H. Krieg, *J. Chem. Phys.*, 2010, **132**, 154104–154123; (*b*) S. Grimme, S. Ehrlich and L. J. Goerigk, *J. Comput. Chem.*, 2011, **32**, 1456–1465.

31 C. Y. Legault, *CYLview, 1.0b*, Université de Sherbrooke, 2009, http://www.cylview.org.

32 (*a*) D. G. Truhlar, B. Garrett and S. J. Klippenstein, *J. Phys. Chem.*, 1996, **100**, 12771–12800; (*b*) J. Lucas Bao and D. G. Truhlar, *Chem. Soc. Rev.*, 2017, **46**, 7548–7596; (*c*) L. Pavlovic, J. Vaitla, A. Bayer and K. H. Hopmann, *Organometallics*, 2018, **37**, 941–948; (*d*) J. M. Crawford and M. S. Sigman, *Synthesis*, 2019, 1021–1036.